Progress of Theoretical Physics, Vol. 72, No. 6, December 1984

Supercritical Behavior of Disordered Orbits of a Circle Map

Kunihiko KANEKO

Department of Physics, University of Tokyo, Tokyo 113

(Received July 4, 1984)

Supercritical behavior of the circle map $x_{n+1}=x_n+A\sin(2\pi x_n)+D$ is investigated. The windows show the similarity in the parameter space (A, D). The critical phenomena of the width of the windows are characterized by the exponent ν, which represents the speed of the collapse of a torus for a given irrational rotation number. Its value is well explained by the RG theory which was originally invented by Feigenbaum et al. and Rand et al. for the subcritical behavior. Next, the notion of "disordering" is introduced to characterize chaotic orbits. The distribution of disordering times is calculated with the use of the induced maps. The distribution shows an exponential decay. The ratio of the decay is related to the instability of unstable cycles. The scaling of the decay is also represented by the exponent ν. A conjecture is proposed that the golden mean torus is the *first* KAM to collapse. Lastly, the period-adding sequence near the crisis and its scaling behavior are studied in the Appendix.

§ 1. Introduction

The mechanism of the transition from torus to chaos has been an important problem in nonlinear studies in recent years. The typical model for the instability in a phase motion is given by a circle map

$$x_{n+1}=f(x_n)=x_n+A\sin(2\pi x_n)+D \quad (\mathrm{mod}\ 1) \tag{1·1}$$

which has been investigated extensively.[2)~12),16)~25)] Especially the critical phenomena near A_c-0 ($A_c=1/(2\pi)$) have been studied intensively. The studies have made clear the following aspects:

i) The lockings form a devil's staircase. The critical phenomena of lockings are analyzed by continued fraction expansions, which show a remarkable change in the convergence rate of the expansions at $A=A_c$.[2)~4)]

ii) The region of lockings to cycles increases as A approaches A_c till the measure of lockings becomes unity at $A=A_c$ (complete devil's staircase).[9)]

iii) The lockings occur via tangent bifurcations, which brings about the similarity of a period-adding sequence. (The similarity holds both for $A>A_c$ and $A<A_c$.)[5)]

iv) The windows for $A>A_c$ form a self-similar structure,[5)~8)] which is studied by the above period-adding analysis[5)] and the locus of superstable periodic orbits (skeletons).[7)]

In the present paper we focus our attention on the supercritical behavior (namely, for $A>A_c$) and study a disordering property of a chaotic orbit (which will be defined in §3). Before going to the detailed study, we note the following properties of the map (1·1) for $A>A_c$.

i) As A is increased from A_c, chaos appears from the locking through usual scenarios (period-doubling[13)] or intermittency[14)] or crisis[15)]). The measure (in the parameter space) of chaos increases for $A>A_c$ with the decrease of the measure of lockings from 1 at $A=A_c$ as is shown in Fig. 1.

ii) The map (1·1) can have two stable attractors for $A>A_c$. The coexistence of two

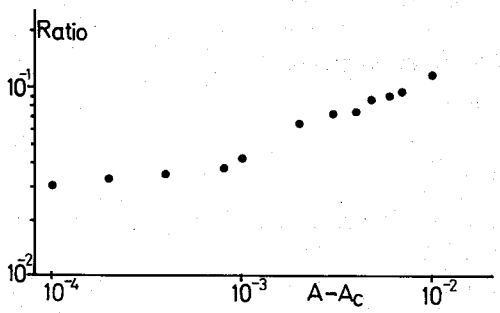

Fig. 1. The ratio of chaotic region in the parameter space D as a function of A. For each (A, D), we have made iterations of the map with the initial value $x_0=0.5$ and regarded the attractor as chaotic if $x_{n+100000} \neq x_{100000}$ for $1<n<50000$ within the error of 10^{-7}. For given A, D is changed from 0 to 0.5 by 2×10^{-3} (for $0.001 \leq A-A_c<0.01$; 250 points of the D's are chosen) or by 10^{-3} (for $A-A_c<0.001$; 500 points) and we have counted the number of the D's for which the attractor is chaotic. The ratio is defined by the number of the D's for chaos divided by 250 (for $0.001 \leq A-A_c<0.01$) or 500 (for $A-A_c<0.001$).

types of cycles or two types of chaos or a cycle and chaos is possible for several parameter regions. The multibasin phenomenon is due to the existence of two critical points (i.e., the points where $f'(x)=0$).

iii) The notion of "ordered" orbits was introduced by Kadanoff.[10] The orbits are in exactly the same order as the orbits for $x_{n+1}=x_n+$(rotation number) and have a simple and beautiful property. The measure for such orbits, however, is zero and almost all orbits are disordered in the sense of §3. Thus, it will be of more importance to study disordered orbits in detail.[11]

The construction of the paper is as follows:

In §2, the phase diagram for the map with $A>A_c$ is given. Especially the similarity of the lockings is examined and the critical phenomena for $A \to A_c+0$ are studied by using the continued fraction expansions for an irrational rotation number.

In §3, the notion of disordering is introduced. It is related to the loss of the ordering of two nearby orbits. In connection with this notion, the distribution of disordering times is defined and analyzed with the use of the induced maps.[16]

In §4, the disordering properties of the orbits near $A=A_c$ are investigated. The slope of the disordering time distribution becomes gentler as A approaches A_c. Its critical phenomenon is studied, in connection with the similarity of chaos with bands with Fibonacci-numbers.

From the arguments in §2 and §4, we can predict the supercritical behavior (the behavior $(A-A_c)^\nu$) of various quantities such as the Lyapunov exponent and the disordering ratio.

Discussions and future problems are given in §5, where multibasin phenomena, future problems on the supercritical phenomena, similarity of chaotic attractors, and noise effect are considered. Especially, the dependence of the speed of the collapse of tori at $A=A_c$ on the irrationality of the rotation number is discussed where a conjecture is made that the golden mean torus is the first to collapse in dissipative mappings.

The crisis frequently appears in the circle map with $A>A_c$ and plays an important role in the change of the disordering property of the orbits in the circle map. In the Appendix, the simplest case of the crisis, i.e., the map $x_{n+1}=1-ax_n^2$ with $a \to 2$ is studied using the induced maps. The period-adding sequence of superstable orbits is chosen to study the similarity of the orbits near the crisis.

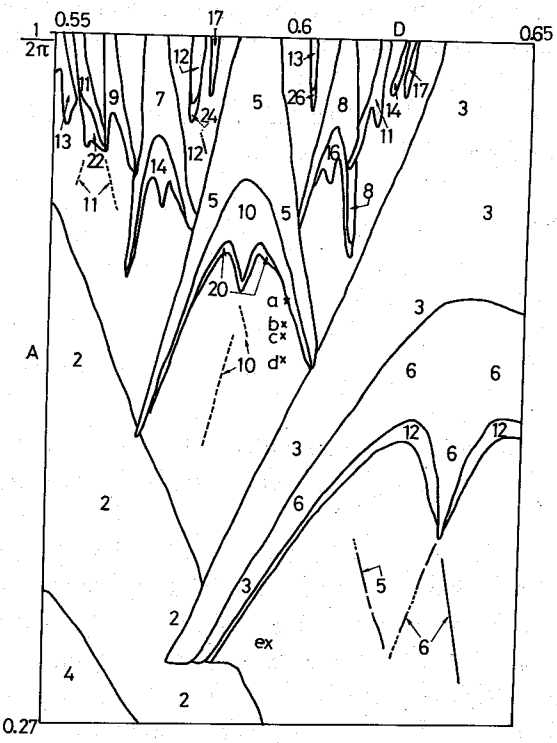

Fig. 2. Rough phase diagram for the circle map. Numbers in the figure denote periods, while chaos exists in the region without numbers. Small structures, such as cycles with periods larger than 26 are omitted. (Initial values of iterations are $x_0=0.5$.)

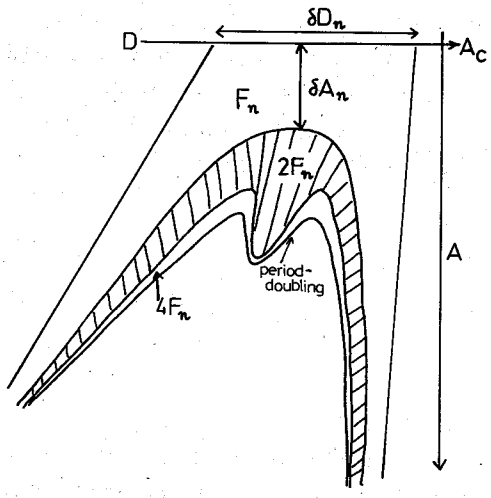

Fig. 3. Schematic representation of the Arnold tongues for $A>A_c$.

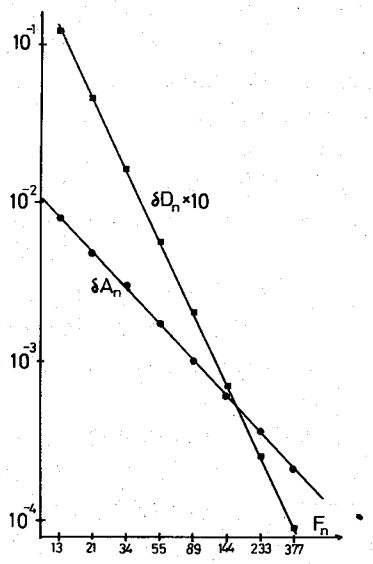

Fig. 4. Log δA_n and log δD_n vs log F_n.

§ 2. Supercritical similarity of the circle map

In Fig. 2, a part of the phase diagram of the map (1·1) for $A>A_c$ is given. Each basic cycle shows period-doublings by the increase of A. The strange figure of each locking (Arnold tongue) is understood from the viewpoint of the cusp bifurcarion.[8] Here we consider the similarity and scaling among lockings in more detail. Each basic locking has a shape like Fig. 3 in the parameter space. The values δD and δA which are defined in Fig. 3, decrease as the period of the basic locking increases. Thus, the chaos appears immediately after A crosses A_c, for a locking with a long enough period. However, the measure of the locking with such a long period is small (i.e., δD decreases rapidly as the increase of the period). The measure of the chaos, therefore, grows up quite slowly, as is seen in Fig. 1.

In order to study the similarity, we consider the sequence of lockings with periods F_n.[2)~4)] Here F_n is chosen to be the Fibonacci sequence (the rotation number is given by F_{n-1}/F_n) which is used as an approximation of the collapse of the golden mean torus.

Here we note that δA is regarded as the index of the onset of chaos, since the chaos from a basic window appears by period-doubling at the parameter about $\delta A(1+\delta^{-1}+\delta^{-2}+\cdots) \propto \delta A$, where δ is Feigenbaum's constant.[13]

Let us study the scaling propeties of δD_n and δA_n which are the values of δD and δA for the lockings with the period F_n. As can be seen from Fig. 4, the relations

$$\delta A_n \propto F_n^{-a} \tag{2·1}$$

and

$$\delta D_n \propto F_n^{-b} \tag{2·2}$$

are obtained with $a=1.055(\pm 0.01)$ and $b=2.165(\pm 0.01)$. The value a is close to the crossover exponent ν, which has been obtained by Shenker[2] and been explained by the RG theory.[3),4)]

The above result is explained as follows: For $A<A_c$ the crossover exponent ν is defined by the postulate that the physical quantities are functions of the single quantity $(A-A_c)F_n^{\nu}$.[2] Thus the above result $\delta A_n \propto F_n^{-a}$ with $a=\nu$ shows that the crossover exponent is the same for $A>A_c$ and $A>A_c$. In generic cases, RG theories have a symmetry for super- and sub-critical regions, which brings about the same value of the exponents for both regions. The above result shows that this symmetry also holds at the fixed point of the RG for the circle map at $A=A_c$.

The exponent b takes the same value as y, where y is the exponent found by S.J. Shenker as the convergence rate of the Fibonacci sequence at $A=A_c$.[2] He chooses cycles which pass $x=0.5$ to determine the exponent y. The above calculation for the exponent b does not use a special choice of a cycle. The agreement with y and b shows that the convergence rate is independent of what orbit we choose (what value of x the cycle passes).

In sum, the Arnold tongues have a similarity also for $A>A_c$, i.e., Fig. 3 takes a similar shape for arbitrary F_n, it it is scaled by Eqs. (2·1) and (2·2). The scaling behavior is characterized by the exponents a and b, the values of which are consistent with the ones obtained by the RG theory for the subcritical region.

§ 3. Disordering of the chaotic orbits

How are the chaotic trajectories characterized? The important difference between chaotic and torus trajectories lies in the "ordering" of trajectories. We call a trajectory "ordered",[10] if the nearby orbits do not change their order. Thus, an "ordered" trajectory cannot fall on the interval $I=\{x|f'(x)<0\}$. The "disordering" means the loss of ordering. That is, the "disordering" occurs when an orbit falls on the interval I, where two nearby orbits change their order*) (see Fig. 5). The disordering of a trajectory in this

*) Preliminary results on the disordering property were reported at the IUTAM conference at Kyoto (1983, September).[11]

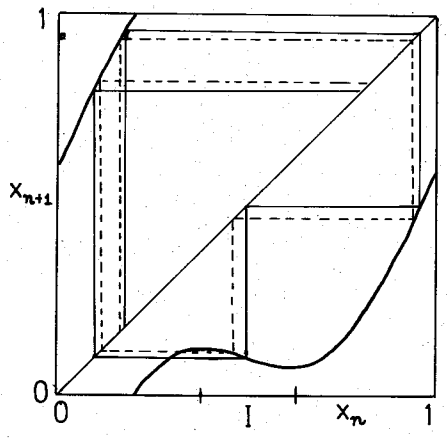

Fig. 5. An illustration of "disordering" of the orbits for the circle map. Two nearby orbits (—— and -----) change their order when they fall on the interval I.

sense is characterized by the ratio that the trajectory falls on the interval I.

We define the disordering ratio d*) by the measure of the orbits in I, i.e., by

$$d=\int_{x\in I}\rho(x)dx\,, \qquad (3\cdot1)$$

where $\rho(x)$ is the probability density, which is defined through a long time average for one orbit which starts with a given initial value.

First, we consider how the chaotic orbit with disordering appears. When the period-doubling bifurcations from a p-cycle to chaos proceed, the disordering ratio changes as

$$1/p=2/(2p)\to 1/(2p)=2/(4p)\to\cdots\frac{2a_{n-1}}{2^{n-1}p}\to\frac{a_n}{2^{n-1}p}=\frac{2a_n}{2^np}\cdots,$$

(↑ doubling) (↑ doubling) (↑ doubling)

where

$$a_n=(2^n-(-1)^n)/3\,.$$

Chaos with the disordering ratio $d\sim 2/(3p)$ is born out of this cascade, which appears in accordance with Feigenbaum's theory.[13] As the nonlinearity A is increased, the disordering property becomes different from the case of a simple logistic map.

In order to study the disordering property in more detail, we introduce here the following induced map $F(x)$ on the interval I:

$$F(x)=f^k(x), \qquad x\in I\,, \qquad (3\cdot2)$$

where k is the minimum integer such that $f^k(x)\in I$. Furthermore, we introduce the distribution $P(k)$ of this "disordering time" k for one orbit with a long time average. Thus,

$$P(k)\propto\int_{x\in I_k}\rho(x)dx$$

holds, where $I_k(\subset I)$ is the region which satisfies $f^k(x)\in I$ and $f^m(x)\notin I$ for $m<k$.

The disordering ratio d is represented in terms of $P(k)$ as

$$d=\sum P(k)/k\,. \qquad (3\cdot3)$$

Examples of the induced maps are given in Figs. 6(a)~(e), while the disordering time distributions (abbreviated as DTD hereafter) are illustrated in Figs. 7(a)~(d). The

*) The disordering also occurs for a periodic orbit for $A>A_c$. Thus, the disordering cannot be an index which distinguishes chaos from a periodic orbit, though topological chaos exists and torus motion is impossible if the disordering ratio is not zero. The disordering ratio is introduced to characterize a chaotic orbit, but it is not related to the Lyapunov exponent.

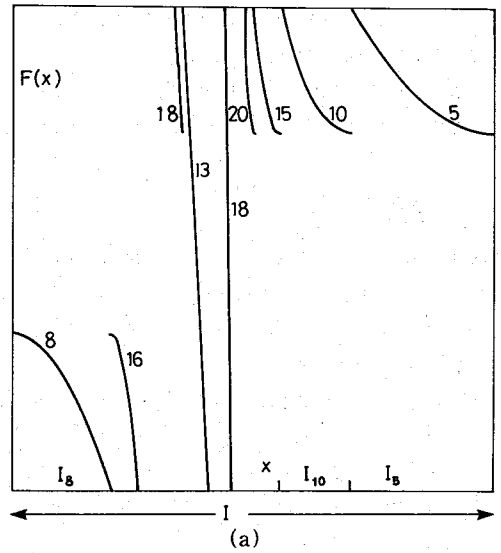

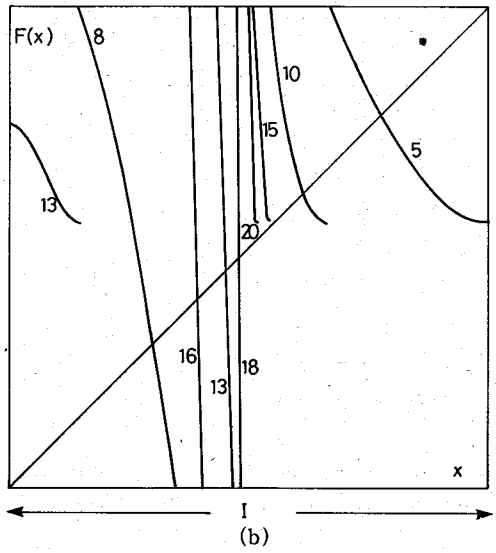

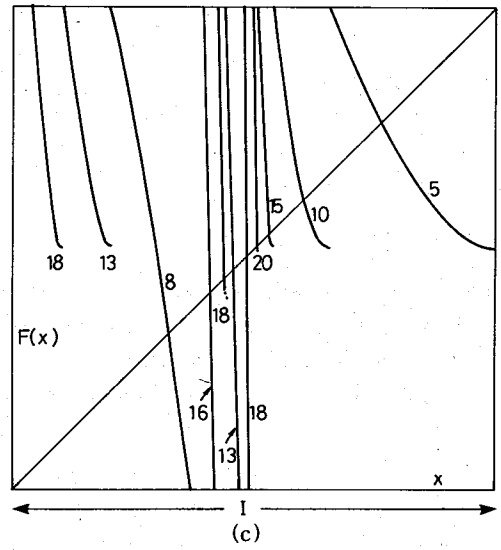

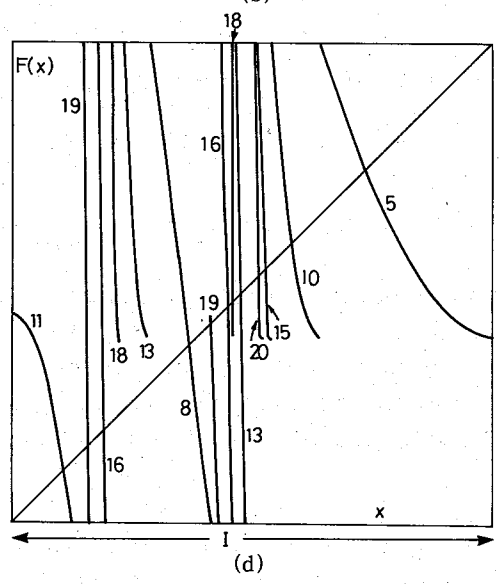

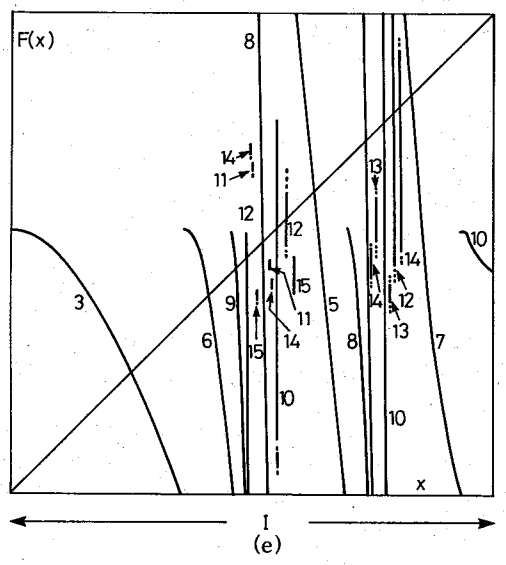

Fig. 6. Induced map $F(x)$ (see Eq. (3·2)) with the disordering time k, where the time k is shown up to 20 for (a)~(d) and up to 15 for (e). D is chosen to be 0.6.

(a) $A=0.196$, (b) $A=0.204$,
(c) $A=0.2058$, (d) $A=0.210$,
(e) $A=0.254$.

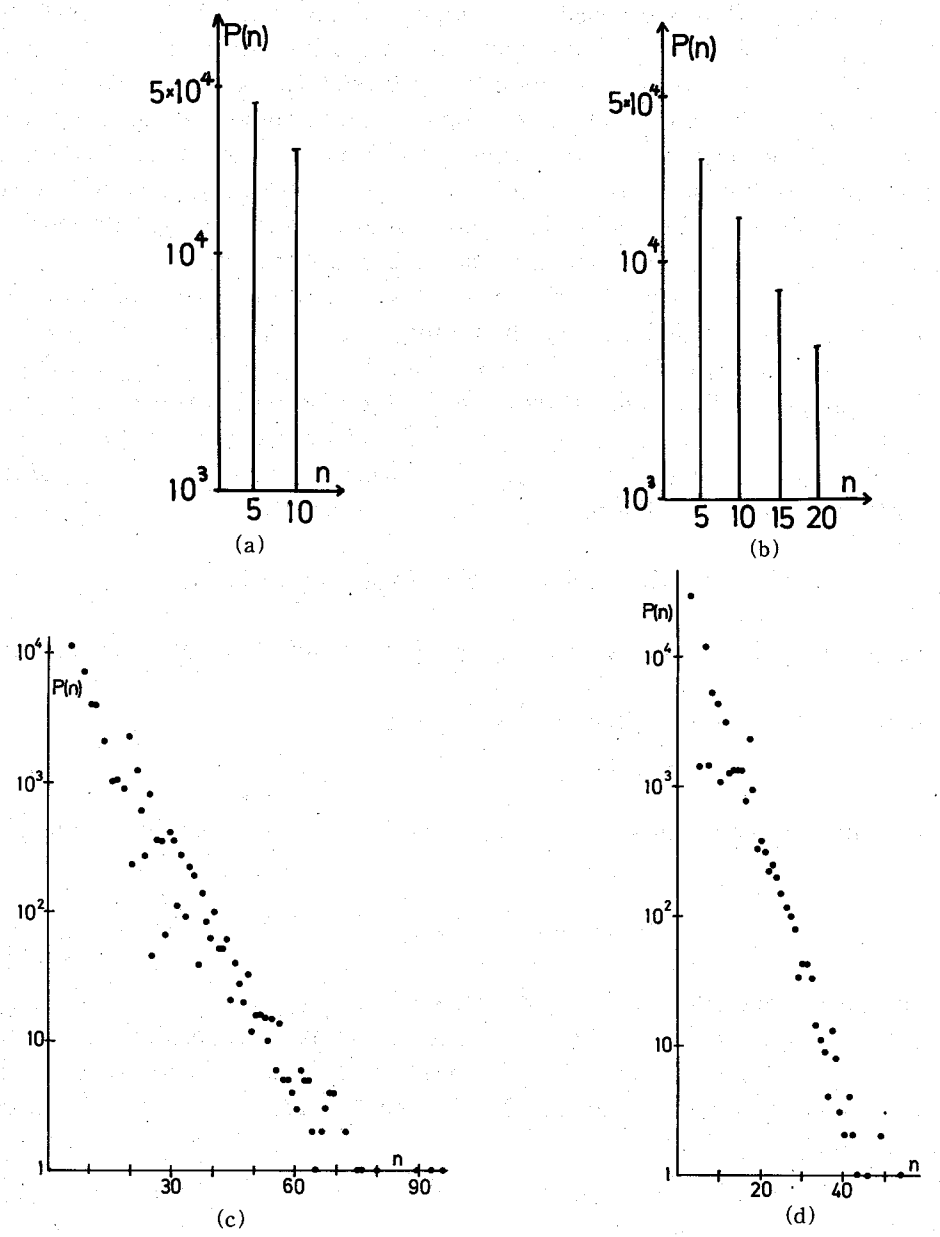

Fig. 7. Distribution of disordering times $P(n)$, which is obtained from 50000 iterations of the circle map with $D=0.6$. (Initial 10000 iterations are dropped.)
(a) $A=0.204$, (b) $A=0.2058$, (c) $A=0.210$, (d) $A=0.254$.

parameter values for these figures are shown in the phase diagram in Fig. 2.

Let us consider the change of disordering properties due to the increase of the nonlinearity A. After the period-doubling bifurcations from a p-cycle are completed, chaos with p-bands appears. As an example we consider the case $p=5$ (with $D=0.6$). Just after the accumulation of doubling cascades, the support of the invariant measure is restricted only in the region I_5 (i.e., in the region $f^5(x)\in I$ and $f^m(x)\notin I$ for $m<5$). See Fig. 6(a) for the induced map. Thus the DTD $P(k)$ is nonzero only for $k=5$.

As the nonlinearity A is increased, the support of the measure inceases into the regions I_5 and I_{10} and $P(k)\neq 0$ for $k=5$ and 10 (see Figs. 6(b) and 7(a)). As the nonlinearity A is increased further, the disordering time $5\times n$ ($n=1, 2, 3, 4, \cdots$) appears successively (see Figs. 6(c) and 7(b) for example) and at some critical point all the disordering times of the form $5\times n$ exist, where the "crisis" of the chaos with 5-bands occurs. The above mechanism of the evolution is independent of p (period of the band). The essential mechanism of the evolution of DTD near the crisis is understood by the logistic map $x_{n+1}=1-ax_n^2$ at $a\sim 2$, which is shown in the Appendix.

After the crisis of a 5-chaos occurs, the orbit can go out of the region $\cup_{n=1}^{\infty} I_{5n}$. When the parameter A is increased and exceeds the region of the doubling cascade of $m\times 2^n$ in the phase diagram, a new disordering time m (and $k\times m$ ($k=1, 2, 3, \cdots$) successively) appears. For example, at the point 'd' (see Fig. 2), the disordering time 8 appears (see Figs. 6(d) and 7(c)). As A is increased further, the disordering times $8n+3k$ appear successively, till the disordering time 3 appears (see Figs. 6(e) and 7(d)). The disordering property evolves in this way as the increase of the nonlinearity.

§ 4. Supercritical behavior of disordering property

Here, we consider DTD and induced maps in more detail, especially focusing on the properties at $A\to A_c$.

As is shown in the Appendix, the DTD behaves as

$$P(nk)\propto \gamma^{-n} \tag{4·1}$$

when the crisis of a k-band chaos occurs. Here, the value γ is given by the instability exponent

$$|f^{k'}(x_i)|=\prod_{i=1}^{k}|f'(x_i)|, \tag{4·2}$$

where x_i is an unstable periodic point (with period k).

Let us take into account the similarity of windows in §2 and consider the case when each F_k-band (F_k is the Fibonacci sequence) chaos shows a crisis. The parameters A and D are taken so that the similarity holds. Then at each value for the chaos with bands with Fibonacci-numbers,

$$P(nF_k)\sim P(F_k)\times \gamma^{-n}, \tag{4·3}$$

where γ is given by the instability exponent of the unstable periodic point with period F_k and γ is expected to approach a constant value as F_k approaches infinity (according to the similarity in §2). Equation (4·3) can be rewritten as

$$P(x)\sim \gamma^{-x/F_k} \tag{4·4}$$

which shows that the slope of DTD approaches $\log 1=0$, taking the form of $-(1/F_k)\log\gamma$, as A goes to A_c. Using the results in §2, F_k may be replaced by $(A-A_c)^{-1/a}$. Thus, the slope of DTD approaches 0 by taking the behavior

$$-(A-A_c)^{1/a}\log\gamma \tag{4·5}$$

when we decrease the value A, changing the value D so that the rotation number is the

inverse of the golden mean.

The exponential decay of the DTD is due to the almost Markov character of the map. At $A=A_c+0$, the decay rate vanishes and the DTD is expected to show *a* power decay. The change from "exponential" to "power" is widely seen in the phase transition. For the intermittent transition, Aizawa et al.[16] have recently found the power distribution of the residence time.

The above analysis is based on the similarity of chaos with F_k-bands. Though we cannot make an accurate argument for an arbitrary point of the parameter space, the following properties should be noted:

1) When the disordering times k and l exist, other times $mk+nl$ ($m, n=1, 2, \cdots$) are apt to exist. If the instability exponents for the unstable k- and l-cycles are given by $\alpha=\prod_{i=1}^{k}|f'(x_i)|$ and $\beta=\prod_{j=1}^{l}|f'(x_j')|$ ($\{x_i\}$ and $\{x_j'\}$ are periodic points for k- and l-cycles respectively), the DTD is given approximately be

$$P(mk+nl)\sim\alpha^{-m}\beta^{-n}. \tag{4·6}$$

2) For an arbitrary cycle with the period k, $P(k)$ is roughly proportional to $\gamma_k^{-1}=|\prod_{i=1}^{k}f'(x_i)|^{-1}$ ($\{x_i\}$ are periodic points).*) Roughly speaking, $\gamma_k\sim\langle|f'|\rangle^k$, where $\langle|f'|\rangle$ is some average of $|f'(x)|$. Since $\langle|f'|\rangle$ is expected to grow as A is increased, the decay rate γ gets larger with the increase of A, as is typically seen in Figs. 7(c) and 7(d) and 8. (Note the change of the scales between Figs. 8(a) and (b). As $(A-A_c)$ is reduced almost to 10%, the decay rate of the slope is also reduced about to 10%, as is seen from these two

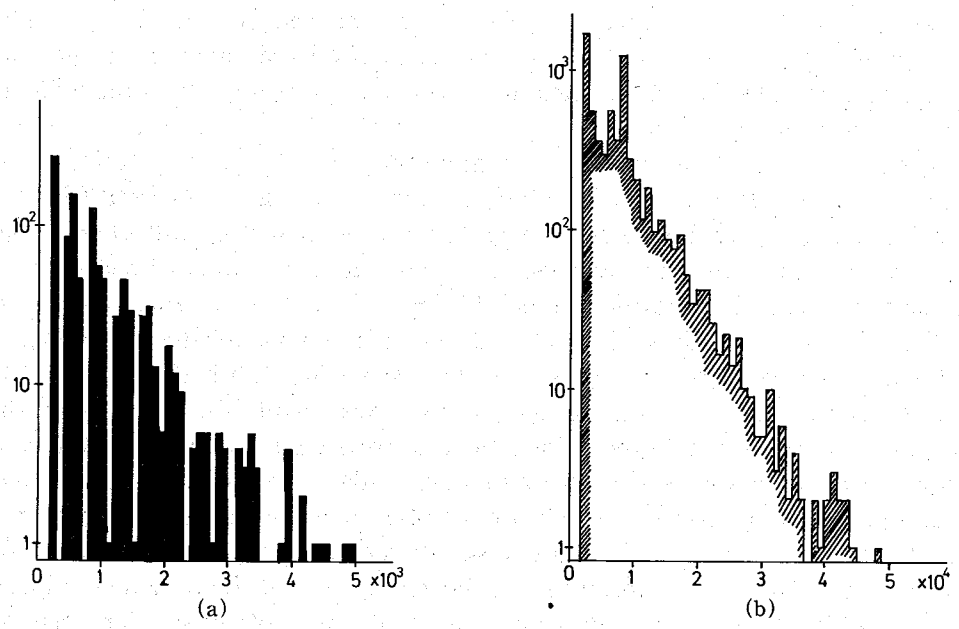

Fig. 8. Histogram of the distribution of disordering times $P(n)$, which is obtained from 10^7 iterations of the circle map. (Initial 10^4 iterations are dropped.)
(a) $A=A_c+0.0008$ and $D=0.6065$: Longitudinal axis is the summation of $P(n)$ for the interval $(n\times10^2, (n+1)\times10^2)$.
(b) $A=A_c+0.0001$ and $D=0.6066$: Longitudinal axis is the summation of $P(n)$ for the interval $(n\times10^3, (n+1)\times10^3)$.

*) The idea to relate the instability exponent with the invariant measure was introduced by Kai and Tomita.[17]

figures.) As A approaches A_c, $\langle|f'|\rangle$ is expected to approach 1. Thus, DTD for the chaos near $A=A_c$ (with arbitrary rotation number) is expected to show the power decay.

Of course, the decay of DTD is not monotonic. It has many peaks and is not simple at all (see Figs. 7 and 8). We also note that smaller disordering times are successively inhibited as A approaches A_c (see Figs. 8(a) and (b)).

3) It will be important to construct a symbolic dynamics $I_j \to I_k$. From the transition probability between the states I_j and I_k, we can understand the disordered property of chaotic trajectories.[18]

§ 5. Discussion and future problems

In the present paper we have investigated the supercritical behavior of chaos after the collapse of tori. To sum up the results:

1) The Arnold tongues have similarity and scalings even for the region $A>A_c$. The scalings are well explained by the RG theory originaly invented for the region $A<A_c$.

2) The chaotic orbits are characterized by the disordering, which is analyzed with the use of the induced maps. As the nonlinearity A is increased, new disordering times appear successively.

3) As A approaches A_c, the smaller disordering times are successively inhibited. Scaling behavior of the disordering time distribution (DTD) is characterized by the crossover exponent ν.

4) The DTD shows almost the Markov character (exponential decay) for $A>A_c$. The decay rate is given by the instability exponent, which approaches 0 as $A \to A_c$. The above exponential decay is well understood for the crisis of k-band chaos in the Appendix.

In connection with the supercritical behavior of a circle map, the following problems are left for future study.

1) The exponents for the subcritical regions depend on the structure of continued fraction expansions of the irrational rotation number. Thus, it is expected that the speed of the collapse of tori (it may be characterized by the exponent a in §2 where $\delta A_n \propto F_n^{-a}$) depends on the irrationality of the torus. According to the results by Shenker,[2] $a=1.0476\cdots$ for the torus with the rotation number $1/(2+(1/2+(1/2+\cdots)$, since $a=\nu$ is strongly suggested in §2 (note that the exponent is smaller than the one for the golden mean torus). Thus, the golden mean torus collapses *faster* than the torus with $1/(2+(1/2+(1/2+\cdots)$ in the above sense, which is quite contrary to the well-established result for the area-preserving mappings,[19] where the golden mean torus is the last KAM to collapse. It will be of importance to check the conjecture that the golden mean torus is the first to collapse in the dissipative mappings (i.e., $a=\nu$ takes its maximum for the rotaion number with the tail of $1/(1+/(1+/(1+\cdots))$. In some sense, the conjecture is rather natural, since the locking with a smaller period collapses at a larger value of A (by period-doublings) in the circle map, while the stochasticity around the resonance with a smaller period plays a more essential role for the collapse of tori in area-preserving systems.

2) Detailed study on the supercritical behavior: In the present paper, only a restricted aspect of the critical phenomena is treated. More accurate study on the increase of the measure of the chaotic regions in the parameter space gives the exponent β, where the measure is given by $(A-A_c)^\beta$. In one sense, the exponent β corresponds to the exponent for the order parameter (Magnetization $(T-T_c)^\beta$ for spin systems) and may be

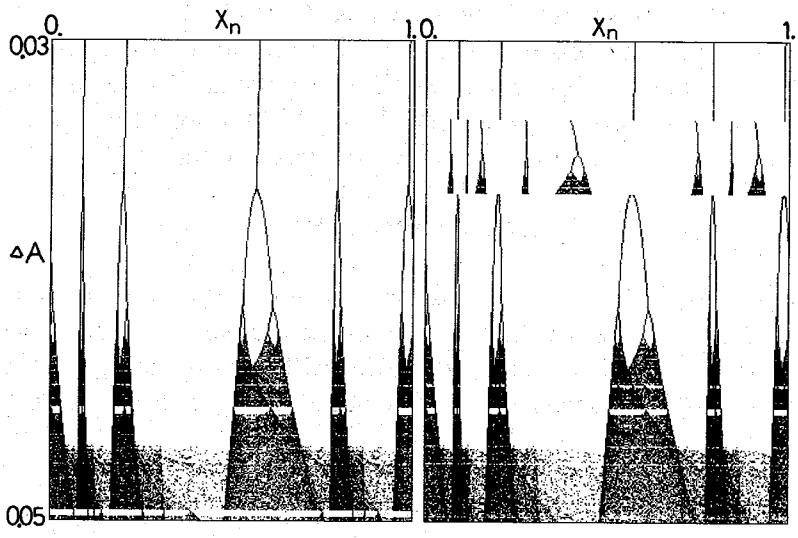

Fig. 9. The orbits x_n for $5000<n<10000$ for the circle map as $\Delta A=A-A_c$ is changed from 0.03 to 0.05. The left figure is for the initial value $x_0=1/(2\pi)\arccos(-1/(2\pi A))$ with $x_0<0.5$ and the right one is for the branch $x_0>0.5$. D is chosen to be 0.6.

independent of the exponents in the subcritical region. The increase of the disordering ratio and the Lyapunov exponent for a given irrational rotation number is expected to show the behavior $(A-A_c)^{1/\nu}$ according to the argument in §4, which has to be checked numerically in the future. The detailed quantitative study on the critical behavior of DTD will also be an important problem.

3) Multibasin phenomena: Since there exist two critical points for the map $f(x)$ for $A>A_c$, two attractors can coexist in some parameter regions. We have already reported an example of the coexistence of two windows in connection with the period-adding sequence. The multibasins can be clearly seen in Fig. 9, where the initial points are given by the two critical points of $f(x)$. The fractal basin strucrure is expected[20] since the topological chaos exists for $A>A_c$. The detailed study is left to the future.

4) Similarity of chaotic attractors: In the present paper only the similarity among the windows is investigated. It is, of course, expected that the similarity structure exists also among chaotic bands. For the chaos between the period-adding windows, the scaling behavior for the Lyapunov exponent has already been reported.[11] In a piecewise-linear mapping, the similarity of chaotic bands was found by Mori et al.[21] It will be of importance to clarify the similarity of chaotic bands for the circle map.

5) Noise effect: The smaller window structures disappear successively by the increase of the noise. The scaling behavior of the visible limit of the windows and the strength of the noise may be expected. In the chaos between the windows, the Lyapunov exponent decreases by the addition of the noise, which will be due to the effect of the nearby windows.

6) Amplitude instability of the torus motion also brings about the collapse of tori, which has recently been studied by many authors as the torus doubling,[22] oscillation of tori,[23] fractalization of tori[24] and torus intermittency.[25] Study of the supercritical behavior of the chaotic orbits after the collapse of tori of these types is also left to the future, which will be characterized by the disordering property, fractal dimension, the width of the

attractor, and the integrated noise of the powerspectra and so on.

Collapse of tori and the onset of chaos have many aspects and seem to be more difficult than the period-doubling scenario for the onset of chaos, which has become one of the greatest success in nonlinear physics in our days.[13] Future efforts will elucidate the detailed mechanism of the collapse of tori and the onset of chaos.

Acknowledgements

The author would like to thank Professor M. Suzuki for useful discussions and critical reading of the manuscript and Mr. S. Takesue for invaluable comments especially on the multibasin phenomena. He is also grateful to LICEPP for the facility of FACOM M190. This study was partially financed by the Scientific Research Fund of the Ministry of Education, Science and Culture.

Appendix

In this appendix, we consider the change of the chaotic orbits near the crisis,[18] using the induced map and the period-adding sequence. The logistic map

$$x_{n+1}=F(x_n;\, a)=1-ax_n^2 \qquad (A\cdot 1)$$

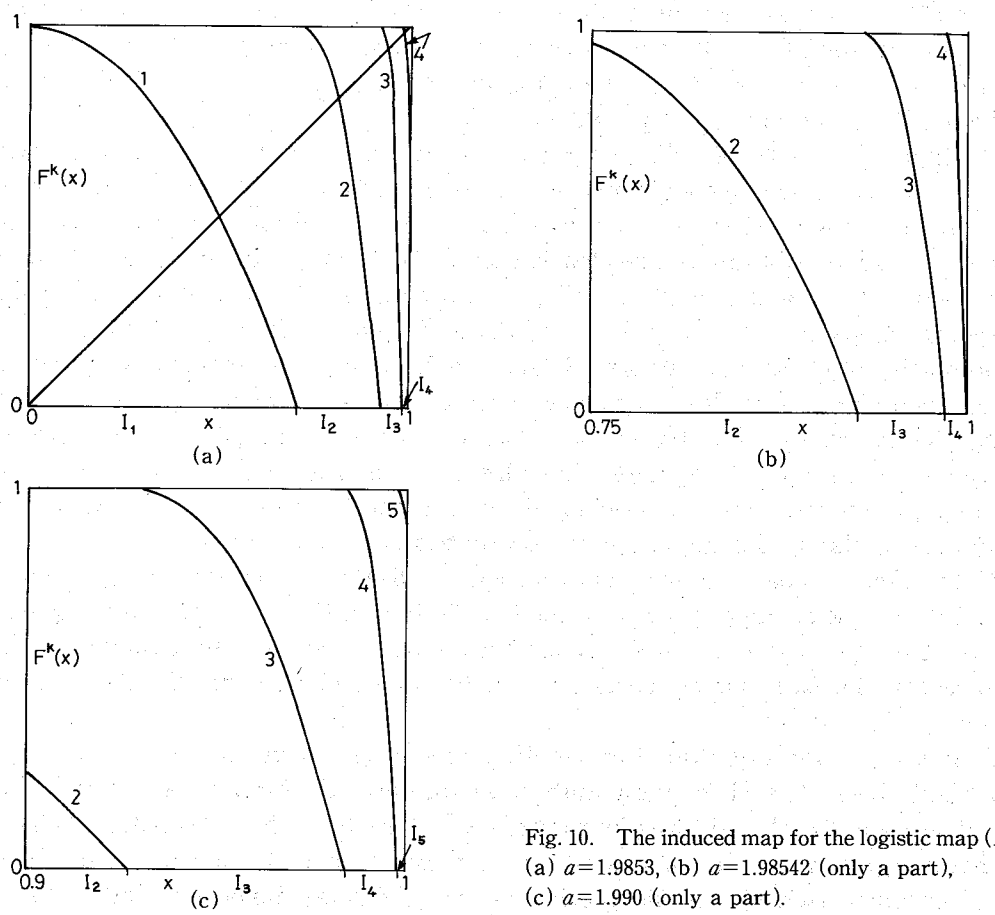

Fig. 10. The induced map for the logistic map (A·1). (a) $a=1.9853$, (b) $a=1.98542$ (only a part), (c) $a=1.990$ (only a part).

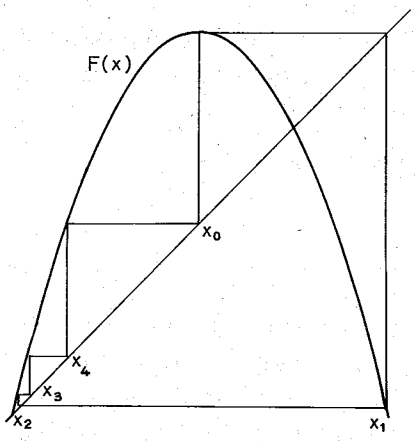

Fig. 11. An example of a superstable orbit at $a=a_4$ $=1.98542\cdots$.

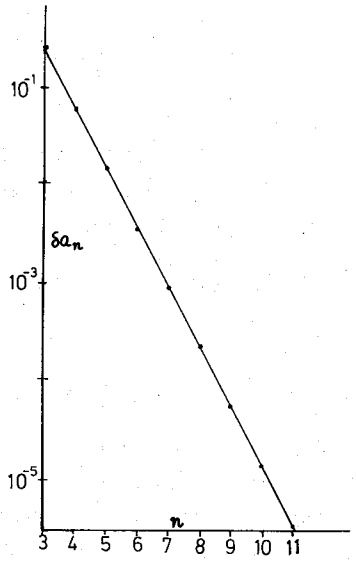

Fig. 12. $\log \delta\ a_n$ vs n for $n=3$ to 11. The slope of the line is $-\log 4$.

near $a=2$ is taken as the simplest and essential case. We construct the induced map for (A·1) by choosing the interval $(0, F(0))$. In Figs. 10(a)~(c), some examples of the induced maps are shown. At $a=a_n$, a new number "n" appears (it corresponds to the disordering time in §3). The orbits for $a>a_n$ and for $a<a_n$ differ in the following sense.

Let us construct the symbolic dynamics by assigning R for $x>0$ and L for $x<0$. For $a<a_n$, the symbolic sequence of an orbit does not contain the sequence of $\underbrace{LL\cdots LL}_{m}$ with $m>n$. At $a=a_n$ a superstable cycle $x_0=0, x_1=1, x_2=1-a,\cdots, x_{n+1}=0$ (see Fig. 11 for an example) appears. For $a>a_n$ a symbolic sequence of the type $R\underbrace{LL\cdots LL}_{n}R$ appears. In this way, the symbolic sequence of the orbits for the map (A·1) approaches the sequence of the coin tossing as n is increased ($a\to 2$). At $a=2$, the symbolic sequence includes all possible (R, L)-sequences (equivalent to the coin tossing), where the crisis occurs.

The superstable cycle at $a=a_n$ is of the type $(0\underbrace{RLL\cdots LL}_{n-1})$, which cooresponds to the cycle with the rotation number $=1/n$ in the circle map. (In the map (A·1), the rotation number corresponds to the ratio of the points at $x>0$.) Between $a=a_n$ and a_{n+1}, there exists a superstable cycle with $kn+m(n+1)$ (k and m are positive integers), which is quite analogous to the construction of the devil's staircase in the circle map. Taking this correspondence into account, we can extract the structure of the devil's staircase (Farey series) from the bifurcation sequence of all unimodal mappings. The Fibonacci- and period-adding sequences in the BZ-map[26] can be regarded as an illustration of the above correspondence.

In the circle map, similarity and scalng of the period-adding sequence are studied in some detail. The scaling property for the period-adding sequence near the crisis is shown easily in the following manner:

At $a=a_n$ and $a=a_{n+1}$ the relations

$$F^{n+1}(x=0;\ a=a_n)=0 \qquad (A\cdot 2)$$

and

$$F^{n+2}(x=0;\ a=a_{n+1})=0 \tag{A·3}$$

hold. Assuming that $\delta a_n=2-a_n$ is small. we have $(\delta a_n-\delta a_{n+1})\propto(A_n+B_n)^{-1}$, where $A_n=\partial F^n(x=1-a_n,\ a=a_n)/\partial x$ and $B_n=\partial F^n(x=1-a_n,\ a=a_n)/\partial a$. Using the chain rules and taking into account the fact that a large number of periodic points are located close to the unstable fixed point $x=-1$ for a large n, we have

$$A_n\propto(F'(x=1,\ a=2))^n,\qquad B_n\propto(F'(x=-1,\ a=2))^n. \tag{A·4}$$

Thus we have

$$\delta a_n\propto(F'(x=-1,\ a=2))^{-n}=4^{-n}. \tag{A·5}$$

In Fig. 12, δa_n vs n is plotted for $n=3,4,\cdots,11$, which agrees with (A·5) quite well. In general, the scaling relation $\delta a_n\propto a^{-n}$ holds, where a is the eigenvalue of the product of Jacobi matrices for unstable periodic orbits which cause the crisis at $\delta a=0$.

We also note that the width of the parameter region where the cycle with the period n stably exists also obeys the scaling relation $(F'(x=-1;\ a=2))^{-n}$.

The length of the interval I_n in the induced maps for $a\to 2$(see Figs. 10 (a)~(c)) is also proportional to $(F'(x=-1;\ a=2))^{-n}$, since the slope of $F^k(x)$ grows as $(F'(x=-1;\ a=2))^k$. The DTD at $a=2$, thus, shows the behavior

$$P(n)\propto(F'(x=-1;\ a=2))^{-n}, \tag{A·6}$$

where $P(n)$ is the ratio of the symbolic sequence $R\underbrace{LL\cdots L}_{n}LR$, which corresponds to the DTD in §3.

The similarity and scaling of the period-adding sequence are useful to characterize the property of chaotic orbits near the crisis.

References

1) D. Ruelle and F. Takens, Commun. Math. Phys. **20** (1971), 167.
S. Newhouse, D. Ruelle and F. Takens, Commun. Math. Phys. **64** (1978), 35.
2) S. J. Shenker, Physica **5D** (1982), 405.
3) M. J. Feigenbaum, L. P. Kadanoff and S. J. Shenker, Physica **5D** (1982), 370.
4) S. Ostlund, D. Rand, J. Sethna and E. D. Siggia, Physica **8D** (1983), 303.
5) K. Kaneko, Prog. Theor. Phys. **68** (1982), 669; **69** (1983), 403.
6) L. Glass and R. Perez, Phys. Rev. Lett. **48** (1982), 1772.
R. Perez and L. Glass. Phys. Lett. **90A** (1982), 441.
7) L. Glass et al., Phys. Rev. **A29** (1984), No. 3.
J. Belair and L. Glass, Preprint (1984) submitted to Physica D.
8) M. Schell, S. Fraser and R. Kapral, Phys. Rev. **A28** (1983), 373.
9) M. H. Jensen, P. Bak and T. Bohr, Phys. Rev. Lett. **50** (1983), 1637.
10) L. P. Kadanoff J.Stat. Phys. **31** (1983), 1.
11) See K. Kaneko, in *Turbulence and Chaotic Phenomena in Fluids*, ed. T. Tatsumi (North Holland).
12) J. D. Farmer and I. Satija, preprint (1984).
13) M. J. Feigenbaum, J. Stat. Phys. **19** (1978), 25; **21** (1979), 669.
14) Y. Pomeau and P. Manneville, Commun. Math. Phys. **74** (1980), 189.
15) C. Grebogi, E. Ott and J. A. Yorke, Phys. Rev. Lett. **48** (1982), 1507.
16) Y. Aizawa, Prog. Theor. Phys. **70** (1983), 1249.
Y. Aizawa and T. Kohyama, Prog. Theor. Phys. **71** (1983), 917.
17) T. Kai and K. Tomita, Prog. Theor. Phys. **64** (1980), 1532.
18) See also J. Guckemheimer, Physica **1D** (1980), 227.
19) J. M. Greene, J. Math. Phys. **9** (1968), 760; **20** (1979), 1183.
20) S. Takesue and K. Kaneko, Prog. Theor. Phys. **71** (1984), 35.

21) H. Mori, H. Okamoto and M. Ogasawara, Prog. Theor. Phys, **71** (1984), 499.
22) A. Arneodo, P. H. Coullet and E. A. Spiegel, Phys. Lett. **94A** (1983), 1.
V. Franceshini, Physica **6D** (1983), 285.
K. Kaneko, Prog. Theor. Phys. **69** (1983), 1806.
23) K. Kaneko, Prog. Theor. Phys. **72** (1984), 202.
24) K. Kaneko, Prog. Theor. Phys. **71** (1984), 112.
25) H. Daido, to appear in Prog. Theor. Phys.
26) J. L. Hudson, M. Haut and D. Marinko, J. Chem. Phys. **71** (1979), 1601.
I. Tsuda, Prog. Theor. Phys. **66** (1981), 1985.